Assembly and Tests of Mechanical Models of the 15 T Nb_3Sn Dipole Demonstrator

C. Orozco, J. Carmichael, I. Novitski, S. Stoynev, A.V. Zlobin

***Abstract*— Within the US Magnet Development Program, Fermilab is developing a 15 T Nb_3Sn dipole demonstrator. Prior to the construction of the real magnet model, short sections and the whole structure were instrumented with strain gauges and assembled to validate the results of structural analysis, check tooling and to gain experience with the assembly of the real magnet components. This paper summarizes the lessons learned from these mechanical models and compares the measured data with the finite element analysis.** [1]

***Keywords*— Dipole magnet, FEA, Mechanical Model**

I. Introduction

US Magnet Development Program (MDP) [1] is developing a 15 T Nb_3Sn dipole demonstrator [2] for a post-LHC Hadron Collider. The magnet design is based on 60-mm aperture 4-layer shell-type coils, graded between the inner and outer layers to maximize the magnet performance. An innovative mechanical structure based on aluminum IC-clamps and a stainless steel skin are used to preload brittle Nb_3Sn coils and support large Lorentz forces at high fields.

The main goal of the mechanical structure is to provide a stable geometry of the coil during magnet assembly and operation. This stability is achieved by applying pre-stress to the coil during magnet assembly and supporting the compressed coil with a rigid structure during the operation.

To study mechanical properties of this structure as well as to optimize the magnet assembly and coil pre-load procedures prior to the construction of the real model magnets, the short section and the whole structure were assembled with iron and aluminum cylinders ("dummy" coils). The clamps and iron laminations were instrumented with strain gauges to monitor stresses during structure pre-loading. This paper summarizes the lessons learned from these mechanical models and compares the measured data with the results of ANSYS calculations.

II. Magnet Design

The mechanical structure of the 15 T dipole demonstrator is shown in Fig. 1. The 4-layer coil assembly is surrounded by stainless steel spacers and supported by a vertically split iron yoke locked by aluminum clamps. The yoke is surrounded by a 12 mm thick stainless steel skin. The IC- clamps interleave with the iron yoke laminations in the top and bottom sectors of the iron yoke. The axial Lorentz forces on the coil ends are intercepted by two thick end plates connected by eight stainless steel tie rods running through the dedicated holes in the iron yoke. The magnet is 1 m long and has 610 mm outer diameter (OD).

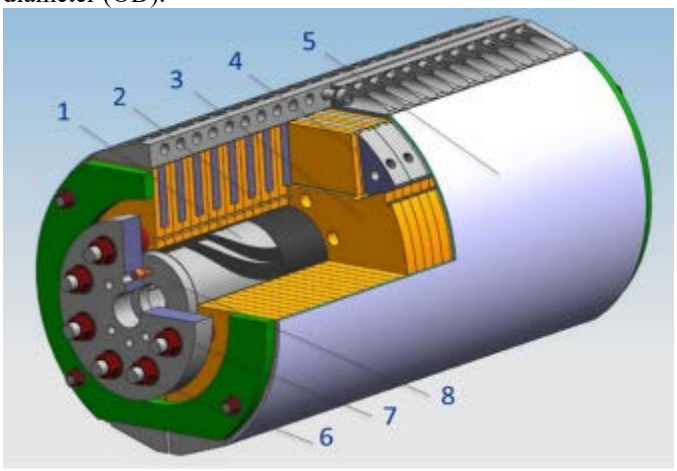

Fig. 1. The 15 T dipole mechanical structure: 1 – Nb_3Sn coil; 2 – coil-yoke stainless steel spacer; 3 – iron lamination; 4 – aluminum clamp; 5 – stainless steel skin; 6 – axial tie rod; 7 – stainless steel end plate; 8 – pusher ring. – *new*

The yoke consists of 84 laminations made of 1020 H.R.S., 42 each on the top and bottom of the assembly. The laminations are held together with 42 clamps made of 7075-T6, 21 each on the sides of the assembly. Four half shells were made of 316 stainless steel.

Based upon prior analysis [2], [3], the program established that a primary area of concern for the mechanical structure are the high stress areas in the iron laminations and clamps (see Fig. 2). The stress in the iron laminations and clamps reaches its maximum at the operation temperature and maximum fields. The calculated values of the equivalent stress at 15 T are shown in Table I. It is known that both iron and aluminum alloy are brittle at low temperature. Since they are key components of the mechanical structure, their mechanical strength is critical.

TABLE I.
FEA RESULTS OF THE DIPOLE MECHANICAL STRUCTURE

	Equivalent stress (MPa)		
	300 K	4 K	15 T
Iron lams	115	353	448
Al clamps	118	280	292

[1] This manuscript has been authored by Fermi Research Alliance, LLC under Contract No. DE-AC02-07CH11359 with the U.S. Department of Energy, Office of Science, Office of High Energy Physics.

C. Orozco, J. Carmichael, I. Novitski, S. Stoynev, A.V. Zlobin are with the Fermi National Accelerator Laboratory, Batavia, IL 60510 USA (e-mail: orozco@fnal.gov).

Summarizing this analysis, the stress concentration results from the gap between the upper and lower laminations, the clamps causing the Laminations to bend around the coil assembly. With this conclusion in mind, the tests performed were designed to induce stress in this area.

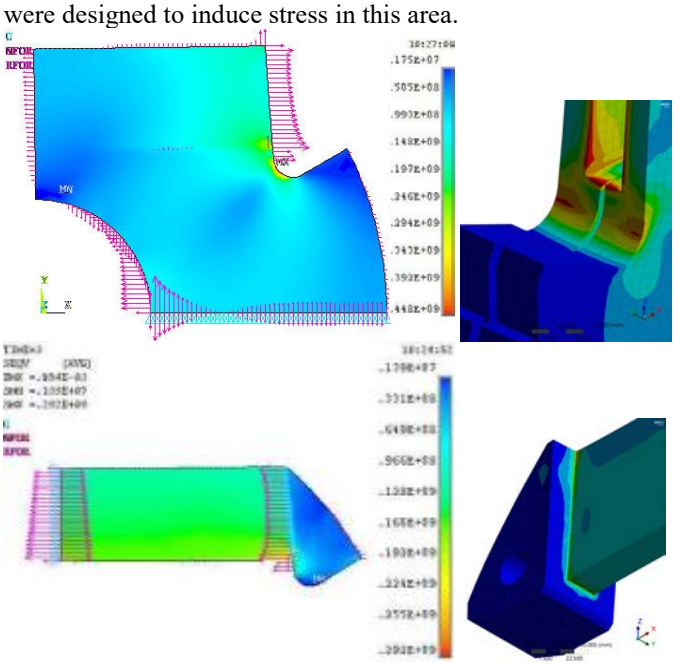

Fig 2: Stress concentration areas, marked in black: lamination (top, right), clamp (bottom, right).

III. Short Mechanical Model

Several versions of the instrumented short mechanical model (MM) were built and tested. The major goal for the MM was to test iron laminations and aluminum clamps (both are brittle at low temperatures). The load was provided using internal support cylinders (aluminum and iron) and various radial shims.

To predict how the cold mass will perform at 4 K and in a field of 15 T, the Short Mechanical Model (SMM), a "cookie" of the cold mass, was used. In the models, the coil assembly is represented by either aluminum or steel cylinders. This shortened structure allows taking more data under varied conditions than it is possible with the entire cold mass due to the cost and time limitations. The specific condition tested here is the SMM's reaction to a liquid nitrogen environment. Further, the cookie can be simulated in a Finite Element Analysis to establish a correlation between the experimental results and the simulation which can then be used to predict stress in the coil assembly.

A. Experimental Setup

The Short Mechanical Model instrumented with strain gauges is shown in Fig. 3. The SMM consists of four laminations, two clamps, four half shells cut to a length consistent with the rest of the SMM, and a dummy coil. For this test, the dummy coil is a 1018 H.R.S. cylinder with an OD consistent with the OD of the coil assembly, thickness 50 mm, and a threaded handling hole in the center. To simulate the magnetic forces the structure will experience when the magnet is powered, shims were placed between the two half shells on each side of the SMM assembly in a roughly 120° arc centered around the pole of the coil assembly. Other than the base case where no shims were used, the SMM was run with 0.127, 0.254, 0.305 and 0.381 mm 316 stainless steel shims.

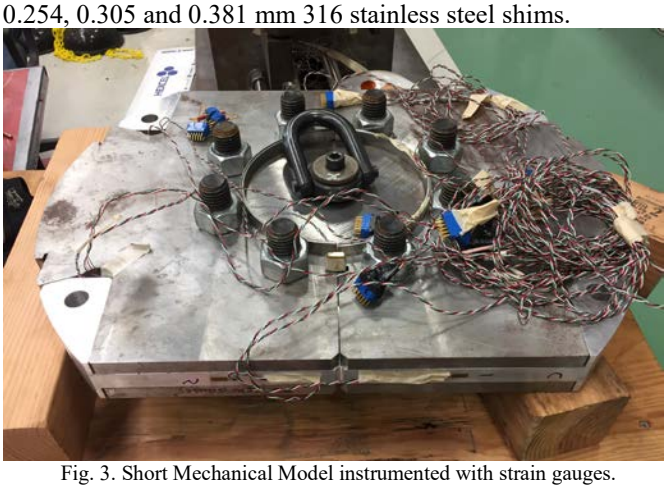

Fig. 3. Short Mechanical Model instrumented with strain gauges.

The SMM were assembled on a workbench using clamps instead of yoking press. Iron lams and clamps are instrumented with strain gauges. Two strain gauges are affixed to each lamination at the lamination stress concentration. Two more strain gauges are affixed to each camp. The clamp gauges are located along the length of the clamp web far from the clamp stress concentration because all flat surfaces near that area are sliding surfaces within the assembly, and thus, any strain gauges applied there would be scraped off during assembly. The strain gauges were read using a QuantumX system manufactured by HBM.

For each shimming configuration, the SMM is set in an aluminum bath sitting on polystyrene blocks. A 160 L dewar of liquid nitrogen is positioned next to the bath and the end of a hose connected to the dewar is placed in the bath, under the SMM. Given the lack of insulation on the bath, the full 160 L is required to bring the model to 77K. Prior to testing of the shimming configurations, each piece of the SMM with a strain gauge was placed in a liquid nitrogen bath to establish baseline measurements of each strain gauge at both room temperature and at 77 K.

B. FEA Setup

ANSYS Workbench 18.2 was used to simulate the SMM. To reduce the necessary computing power, we took advantage of the inherent symmetry in the structure and modeled only a quarter of the SMM (Fig. 4). The shim was modeled as a protrusion on the OD of the inner half shell. Material properties were obtained from Matweb.com. A symmetry condition was placed on the clamp and the dummy coil in the YZ plane. In the XY plane a frictionless support was used to mimic symmetry. This support was applied to the lamination, the half shells, and the dummy coil. The contacts between each of the components were frictional with a friction coefficient of 0.2. For each shimming configuration, the simulation was run for both room temperature and cryogenic temperature.

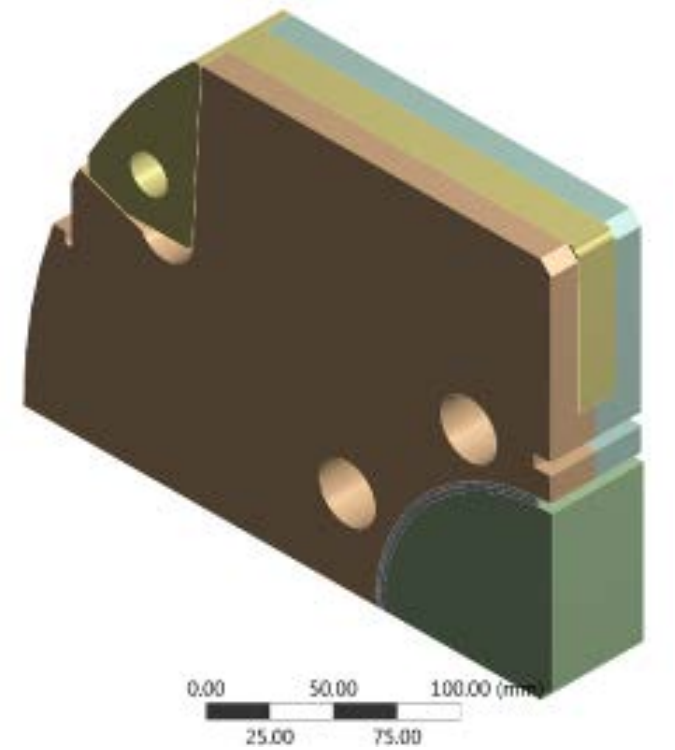

Fig. 4: 3D FEA Model showing quarter geometry and symmetry planes.

Two relevant values were provided by the FEA. The first is the value of equivalent stress in the lamination stress concentration; the second is the value of equivalent stress in the web of the clamp at the position of the strain gauges on the experimental setup.

C. Results

Figures 5 and 6 are the primary results of the SMM. The solid lines represent data from the experimental setup while the dotted lines represent data from the FEA. The lower data sets represent data taken at room temperature while the upper data sets represent data taken at the cryogenic condition. The FEA data appears to correlate well with experimental data for both the laminations and the clamps, with the FEA data often predicting the higher end of the experimental range. One can conclude that the FEA represents a conservative estimation of the stresses in the mechanical structure.

There are, however, a couple anomalies to consider. The first is regarding the outliers in the experimental lamination data at the 0.254 mm shim. These three data are likely the result of a wiring mismatch or physical damage to the gauges themselves. Either way, these data can safely be excluded from the conclusions drawn. The other anomaly is regarding the spread of the cold lamination data with no shim. This is likely due to that data being taken over several months, possibly resulting in drift in the strain gauges. The majority of the experimental data, including the baseline values used to compensate for the gauges' intrinsic initial values, was taken in a three-week period, and the data taken earlier represent the higher end of the spread, so we may softly conclude that this data is evidence of a systematic error not yet accounted for.

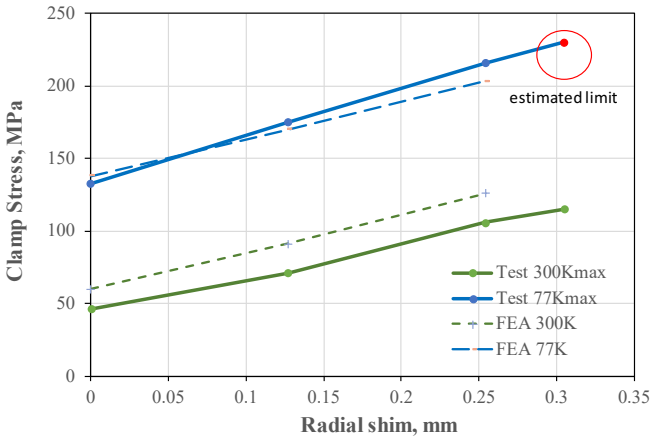

Fig. 5. Experimental and FEA data for clamps vs. the radial shim size.

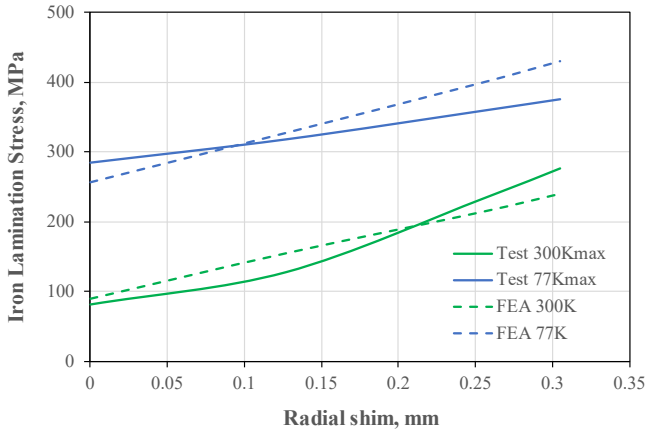

Fig. 6. Experimental and FEA data for laminations vs. the radial shim size.

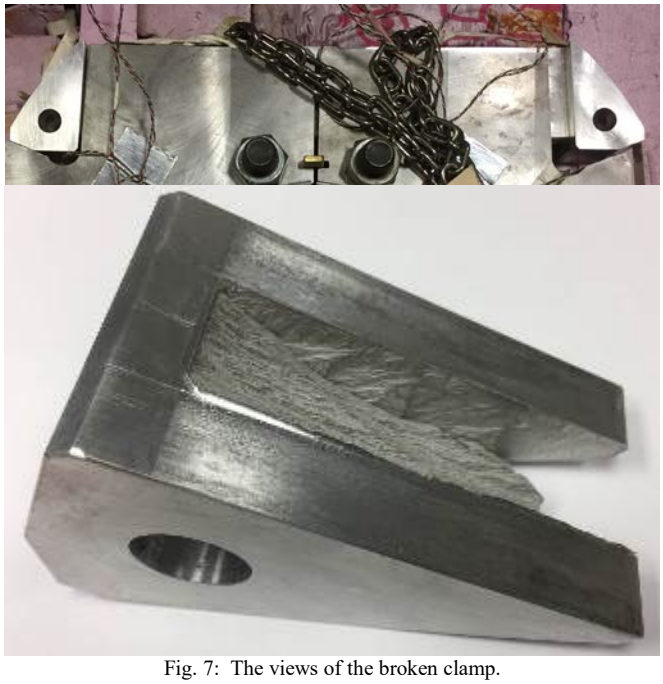
Fig. 7: The views of the broken clamp.

Figures 5 and 6 show data for the 0.305 mm shim only for the warm condition. This is due to the failure of the clamps during testing at that condition (Fig. 7). Without further study,

it is difficult to ascertain the exact propagation of the crack that resulted from the failure, however, it is evident that there are two areas of concern. The first is the sharp corner on the bottom of the web where it connects to the end of the clamp. This corner is a stress concentration that evinces a lipping consistent with the possibility that this is where the crack originated. The second is the propagation of the crack from the plane where the web meets the end to the holes in the end of the clamp. This suggests that the material in the clamp ends is too thin with the existence of the holes.

Based on these results, the clamp design was modified including the larger radius around the entire perimeter in the plane where the web meets the end, and elimination of holes in the ends. The corresponding edges of the laminations were modified accordingly. The SMM with the new clamps and the modified laminations will be assembled and tested.

IV. Long Mechanical Model

The main goals of the Long Mechanical Model included: a) testing all the components of the mechanical structure and assembly tooling, b) developing a magnet assembly plan and pre-stress targets, c) checking instrumentation, d) validation FEA. Model tests included several assemblies with various radial shims and Fuji film between the dummy coil and the iron yoke.

During the assembly, the 42 laminations on the bottom are placed into the lower press tooling. The bottom pair of half shells is set in the pocket formed by the laminations. The coil assembly (or solid cylinders as described above) is set in the lower half shells. The top pair of half shells are place on top of the coil assembly and covered by the other 42 laminations. The upper press tooling is then set atop the upper laminations. The 42 clamps are then partially inserted by hand, which is possible due to the tapered interface between the clamps and the laminations. The structure is then subjected to vertical pressure of up to 34 MPa while the clamps are pressed in by means of a pusher bar which uses two hydraulic cylinders to apply up to 69 MPa to each clamp to force it into position. The vertical pressure is the released.

Figure 8 shows the Long Mechanical Model assembled with instrumented aluminum cylinders (dummy coil) and placed in between the top and bottom tooling outside (left) and in the press with pusher bars (right).

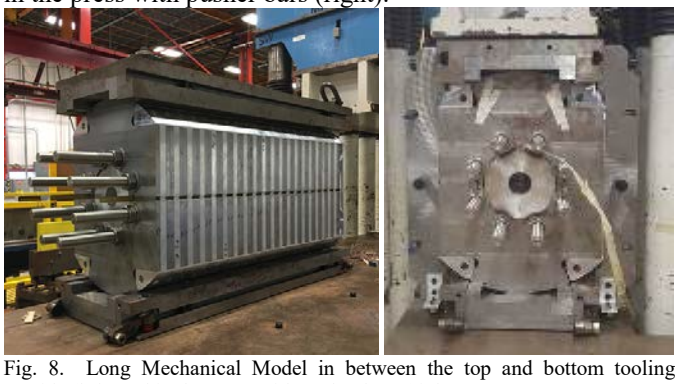

Fig. 8. Long Mechanical Model in between the top and bottom tooling outside (left) and in the press with pusher bars (right).

Figure 9 shows the results of a test conducted with Fuji film. This test allowed us to characterize the Laminations according to their ID, so that we may reorder them to provide for a better stress distribution across the coils.

Fig. 9. Axial radial force distribution measured using Fuji film.

V. Conclusion

Several instrumented mechanical models were built prior to the assembly of the 15 T dipole demonstrator to verify the design concept of the magnet support structure, measure stresses in the key structural components, and to validate FEA results. Based on the results of the SMM and the LMM, we are confident that the mechanical components are sound and that they can be used in in the final 15 T cold mass assembly.

Acknowledgment

The authors would like to thank S. Johnson, J. Karambis, J. McQueary, E. Ruiz, A. Rusy for their contribution to model fabrication and testing.

VI. References

[1] S. Gourlay, S. Prestemon, A. Zlobin, L. Cooley, D. Larbalestier, "The U.S. Magnet Development Program Plan," U.S. Magnet Development Program, Lawrence Berkeley National Lab, Berkeley, CA, USA, Jun. 2016.

[2] I. Novitski, N. Andreev, E. Barzi, J. Carmichael, V. V. Kashikhin, D. Turrioni, M. Yu, and A. V. Zlobin, "Development of a 15 T Nb_3Sn Accelerator Dipole Demonstrator at Fermilab," IEEE Trans. on Appl. Supercond., v. 26, Issue 4, June 2016, 4001007.

[3] C. Kokkinos , I. Apostolidis, J. Carmichael, T. Gortsas, S. Kokkinos, K. Loukas, I. Novitski, D. Polyzos, D. Rodopoulos, D. Schoerling, D. Tommasini,.and A.V. Zlobin, "FEA Model and Mechanical Analysis of the Nb_3Sn 15 T Dipole Demonstrator," IEEE Trans. on Appl. Supercond., v. 28, Issue 3, April 2018, 4007406